Large-Scale Terahertz Active Arrays in Silicon Using Highly-Versatile Electromagnetic Structures

Cheng Wang*, Zhi Hu, G. Zhang, J. Holloway and Ruonan Han (* Email: wangch87@mit.edu)

Department of Electrical Engineering and Computer Science
Massachusetts Institute of Technology, Cambridge, MA, 02139, USA

***Abstract*—The high integration capability of silicon technologies, as well as the small wavelength of terahertz (THz) signals, make it possible to build a high-density, very-large-scale active THz array on a single chip. This is, however, very challenging in practice, due to the low device efficiency and large footprint of conventional circuit designs. To address these problems, we introduce a set of compact while versatile circuits, which utilize the multi-mode behaviors from structures with tight device-electromagnetic integration. These circuits have enabled large-scale (1) homogeneous arrays for high-power, collimated radiation, and (2) heterogeneous arrays for fast broadband spectral scanning. In particular, 0.1-mW power generation (20-mW effective isotropically-radiated power) at 1 THz, simultaneous transmit/receive capability, and high-parallelism molecular spectroscopy are demonstrated. New opportunities that these works bring about are also discussed.**

***Index Terms*—terahertz, large-scale array, radiation, spectroscopy, CMOS, SiGe**

I. Introduction

For the past two decades, the operation frequency of silicon-based devices and circuits has extended from microwave (a few GHz) to millimeter-wave (30∼300 GHz), and in recent years to terahertz regime. The evolution of associated circuit design methodology plays an important role in support of such progress. At microwave frequencies, lumped elements are almost exclusively used. At mmWave frequencies, the smaller wavelength (λ) opens up the opportunities to implement chip-integrated distributed elements, resonant antennas, and other complex structures that manipulate electromagnetic waves [1].

In the THz regime, one exciting opportunity is that very-large-scale, coherent radiation array could, in theory, be built on a single chip. To avoid grating lobes from wave interference of an array, the optimum unit pitch is $\lambda/2$; accordingly, over one thousand radiators at 1 THz can be integrated in a 10-mm^2 chip, generating a beam with only a few degrees of divergence (Fig. 1). Such a property can greatly help compensating the large path loss of THz signals and lead to excellent 2D spatial resolution in imaging. On the other hand, however, the speed plateau of solid-state devices ($f_{max,Si}$≈0.5 THz) leads to large power consumption of THz circuits; and the commonly-used nonlinear operations conventionally require dedicated structures for signal processing (generation, filtering, radiation, etc.) at various harmonic frequencies, which occupy a much larger area than $\lambda/2\times\lambda/2$. It is therefore evident that compact while versatile THz circuit structures are highly desired.

In addition to arrays with uniform, coherent radiator operations (i.e. homogeneous array), heterogeneous arrays can also benefit from such structures. Instead of working collaboratively at the EM level, units of a heterogeneous array perform different domains of signal processing with high parallelism, providing great advantages such as rapid, broadband sensing and channelized tera-scale communication. In this paper, compact, versatile circuit structures are presented, along with SiGe and CMOS prototypes of large-scale active THz arrays.

II. Homogeneous Array: A 1-THz Radiation Source

Sensing with mid-THz (∼1 THz) wave has great potentials in rotational-vibrational spectroscopy for large biological molecules, sub-μm vibrometry and high-resolution imaging. Previously, individual frequency multipliers using high-order harmonics were used to reach 1 THz [2], leading to small output power level (<10 μW). Mid-THz radiation arrays enabling power combining were not reported because: (1) the allowable size of each radiator element is very small ($\lambda/2\times\lambda/2$≈100×100 μm^2 in dielectrics), and (2) a multiplier array requires a centralized network to distribute input signals, with equal phase and amplitude, to each element; given its large size (hence large loss and routing complexity), it is very challenging (if not impossible) to implement such a network.

Using the IHP 130-nm SiGe HBT process (f_{max}=450 GHz), we demonstrate a 1-THz source integrating 91 coherent antennas inside 1-mm^2 area [3]. The enabling technology for such a large-scale array is a self-oscillating radiator structure (Fig. 2), which performs 250-GHz differential oscillation, inter-radiator 2D coupling and 1-THz on-chip radiation *simultaneously*. The equivalent circuit for the 250-GHz oscillation is shown in Fig. 3, where a two-section transmission line behaves as the oscillation feedback path, and the oscillation frequency is regulated by two $\lambda/4$ slot resonators in parallel. We show that by properly selecting the characteristic impedance and length of the feedback path (Z_0 and φ_1+φ_2 in Fig. 3), signal phase delay due to the finite device transit time can be compensated, and maximum oscillation power is achieved [4]. A "flipped microstrip line" is used as one section of the feedback, where lower metal layers are used as the signal trace to avoid loss of vertical vias stacked on top of the HBTs. A slotline is used as another feedback section: it prevents the leakage of the common-mode 1-THz signal from the collectors to the lossy bases through its cutoff behavior for the associated TM wave.

The $\lambda_{f_0}/4$ resonators (f_0=250 GHz) are multi-functional, and their slot structures are bent so as to introduce near-field interference at f_0∼4f_0. As Fig. 4 shows, the standing

waves formed inside each slot section (e.g. *A*-*B*) at f_0, $2f_0$ and $3f_0$ have adjacent *out-of-phase* counterparts in either the horizontal or vertical direction. Undesired radiations at these frequencies are therefore canceled without additional filters. At $4f_0$, the waves in all horizontal slots are *in phase*, which then induce efficient backside radiation through an externally-attached, hemispheric silicon lens (with a simulated efficiency of 63%). No dedicated antenna is required. Lastly, the bent slot resonators are also shared among adjacent radiator units, leading to strong 2D coupling and negligible phase mismatch among units. The self-sustaining nature and compact size of the radiator enable high array scalability and quasi-optical power combining of a large number (84 in [3]) of transistors.

The chip consumes 1.1 W of DC power. The down-converted spectrum of the weak radiation leakage at fundamental frequency is shown in Fig. 5(a), verifying that the 4^{th}-harmonic radiation is at 1.01 THz. Through a WR-1.0 diode detector, the radiation at 1.01 THz is characterized (Fig. 5(b)). 24-dBi directivity and 20-mW equivalent isotropic radiated power (EIRP) are obtained thanks to the large array size. The total radiated power measured by a photo-acoustic power meter is 80 μW – 10x higher than the prior arts in silicon.

III. Heterogeneous Array: Comb Spectrometer

Versatile circuits using high-order device-EM interactions also make large heterogeneous arrays possible. Such arrays offers high-parallelism operations, but previously involve high integration complexity and power consumption. In [5], we demonstrate a bilateral, frequency-comb-based spectroscopy setup, which provides a wide gas-detection range by probing the unique rotational modes of molecules. Instead of the conventional single-tunable-tone scheme, 20 equally-spaced tones are used to scan a 220 to 320-GHz band simultaneously (Fig. 6). Such a comb spectrum is realized by 10 cascading units (Active Molecular Probe AMP in Fig. 7) with simultaneous transmit/receive capability at different channel frequencies. The entire spectrometer is implemented on a single chip using TSMC 65-nm CMOS (f_{max}=250 GHz) with only 6-mm^2 area.

The AMP core (Fig. 8) plays the following roles: (1) frequency doubler for an input fundamental signal at f_{TX}/2, (2) on-chip antenna of the generated signal at f_{TX}, and (3) heterodyne down-mixer of the external incident wave at $f_{TX}\pm f_{IF}$, where f_{IF} (<1 GHz) is the intermediate frequency. For optimal frequency doubling efficiency, the power gain of the transistors at f_{TX}/2 should be maximized. Fig. 8 presents the operations for achieving this goal, where a device feedback network is formed by two transmission lines *TL*1 and *Slot*2. We show that by setting their impedances (Z_{TL1}, Z_{TL2}) and electrical lengths (Z_{φ_1}, Z_{φ_2}) according to the equations in Fig. 8 [6], the device power gain reaches its theoretical limit near G_{max}=4U, where U is the unilateral gain [7]. It is also noteworthy that the functions of *Slot*1 and *Slot*2 are twofold: for differential input signal at f_{TX}/2, *Slot*1 creates feedback and *Slot*2 creates resonance for maximum drain voltage swing; for common-mode signal at f_{TX}, *Slot*1 cuts off the feedback path to reduce loss at gates, and *Slot*2 acts as a folded slot antenna for radiation (Fig. 9). Lastly, since the antenna is reciprocal, an incident wave at $f_{TX}\pm f_{IF}$ is coupled into the heavily-driven transistor pair, which behaves as a sub-harmonic mixer. The down-converted signal at f_{IF} is then extracted from the top of the AMP core (Fig 9).

For a seamless coverage of the 220 to 320-GHz band, each AMP only needs to have 10-GHz tuning range. Compared to the single-tone spectrometer, this maintains peak performance across the entire band. In measurement, a total radiated power of 5.2 mW and a noise figure of 14.6 to 19.5 dB are obtained (Fig. 10∼Fig. 12). Meanwhile, the 20-channel parallel operation, in conjunction with the higher signal-to-noise ratio (SNR) that the system delivers, reduces the total scanning time by approximately ∼100× [6]. As a result, the energy consumption of the system is significantly decreased. With the chip DC power of 1.7 W, an excellent spectral sampling efficiency of 0.17 mJ/point (τ=1 ms) is achieved.

An experimental setup for gas sensing using the CMOS spectrometer is shown in Fig. 13, where the gas sample pressure is reduced below 10 Pascal to eliminate the spectral-broadening effect due to the inter-molecular collision [8]. In Fig. 14, absorption spectral lines of carbonyl sulfide (OCS) located in the 220-to-320-GHz band, as well as the zoom-in details of one line near 279.685 GHz, are shown[1] [9]. The narrow linewidth (∼1 MHz) leads to ultra-high specificity for gas mixture analysis. High $\text{SNR}_{v/v}$ is achieved for pure molecular gas (Fig. 15) and scales linearly with molecular concentration, leading to a detection sensitivity (lock-in bandwidth=1 Hz) of 11 *ppm* for OCS. For molecules with smaller mass or larger dipole moment, even higher sensitivity can be provided (e.g. 3 *ppm* for hydrogen cyanide HCN). With gas pre-concentration, the sensitivity can be further improved to 10∼100-*ppt* level, enabling breath analysis, industrial-process monitoring and potentially trace-gas sensing.

IV. Conclusions

We show that the large integration capability of silicon processes not only enables monolithic "*THz+Analog+Digital*" systems, but also greatly enhances THz-circuit performance itself when new versatile structures and distributed/parallel architectures are adopted. The inferior speed performance of silicon devices can then be well compensated in a systematic context. Given the high scalability of the presented work, >1 mW power generation and a few hundred GHz coverage around 1 THz should be possible in the near future. Lastly, we also note that all techniques presented here also apply to III-V (InP, GaN...) devices and III-V/Si heterogeneous platforms, which are expected to deliver even better performance.

V. Acknowledgements

We acknowledge the support from NSF, MIT Lincoln Labs, ADI, TSMC, and Singapore National Research Foundation.

[1]A standard wavelength modulation is applied to the comb spectrum to reduce the impact of standing waves, as a result, the measured plot is close to the first-order derivative of the absorption spectral line.

REFERENCES

[1] A. Hajimiri, "The Future of High Frequency Circuit Design," in *Proc. of the European Solid State Device Research Conf.*, 2009.

[2] Z. Ahmad, M. Lee, and K. K. O, "1.4THz, 13dBm-EIRP Frequency Multiplier Chain Using Symmetric- and Asymmetric-CV Varactors in 65nm CMOS," in *IEEE Intl. Solid-State Circuits Conference (ISSCC)*, pp. 350–351, 2016.

[3] Z. Hu and R. Han, "Fully-Scalable 2D THz Radiating Array : A 42-Element Source in 130-nm SiGe with 80-uW Total Radiated Power at 1.01 THz," in *IEEE Radio-Frequency Integrated Circuit Symposium*, (Honolulu, HI), 2017.

[4] R. Han, C. Jiang, A. Mostajeran, M. Emadi, H. Aghasi, H. Sherry, A. Cathelin, and E. Afshari, "A SiGe Terahertz Heterodyne Imaging Transmitter with 3.3 mW Radiated Power and Fully-Integrated Phase-Locked Loop," *IEEE Journal of Solid-State Circuits*, vol. 50, no. 12, pp. 2935–2947, 2015.

[5] C. Wang and R. Han, "Rapid and Energy-Efficient Molecular Sensing Using Dual mm-Wave Combs in 65nm CMOS: A 220-to-320GHz Spectrometer with 5.2mW Radiated Power and 14.6-to-19.5dB Noise Figure," in *International Solid-State Circuit Conference (ISSCC)*, (San Francisco, CA), pp. 18–20, 2017.

[6] C. Wang and R. Han, "A Dual-Terahertz-Comb Spectrometer on CMOS for Rapid, Wide-Range Gas Detection with Absolute Specificity (Invited)," *IEEE Journal of Solid State Circuits*, 2017.

[7] R. Spence, *Linear Active Networks*. John Wiley & Sons Ltd, 1970.

[8] C. H. Townes and A. L. Schawlow, *Microwave Spectroscopy (Dover Books on Physics)*. 2nd ed., 2012.

[9] C. Wang and R. Han, "Molecular Detection for Unconcentrated Gas with ppm Sensitivity Using Dual-THz-Comb Spectrometer in CMOS," *invited and submitted to IEEE Trans. Biomedical Circuits and Systems*, 2017.

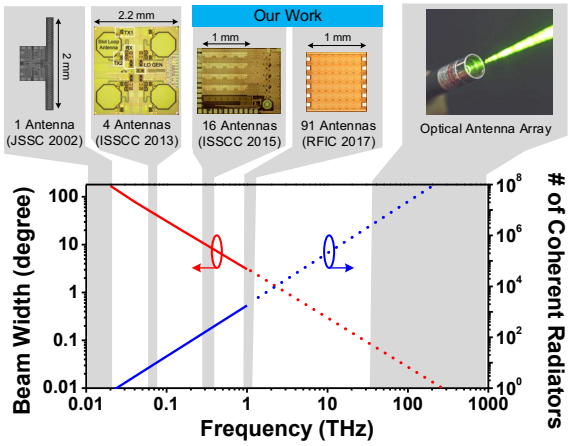

Fig. 1: Estimated beam width and number of coherent radiators (pitch=$\lambda/2$) inside a 10-mm^2 chip area. A few prior arts at varying frequencies matching such radiator densities are also shown.

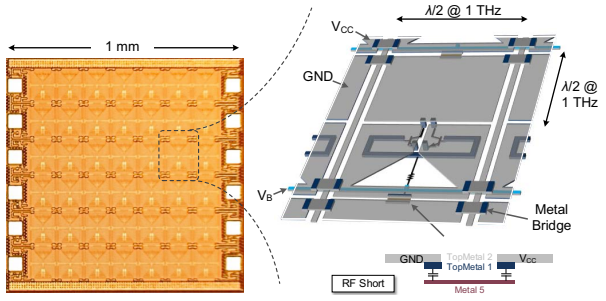

Fig. 2: Die photo of the 1-THz radiation source in 130-nm SiGe process and the 3D structure of the radiator unit.

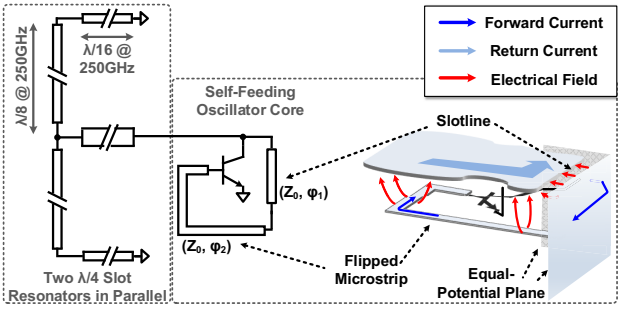

Fig. 3: Half-circuit equivalent of the self-oscillating radiator at fundamental frequency (250 GHz), as well as the structure and field distribution of the oscillator core.

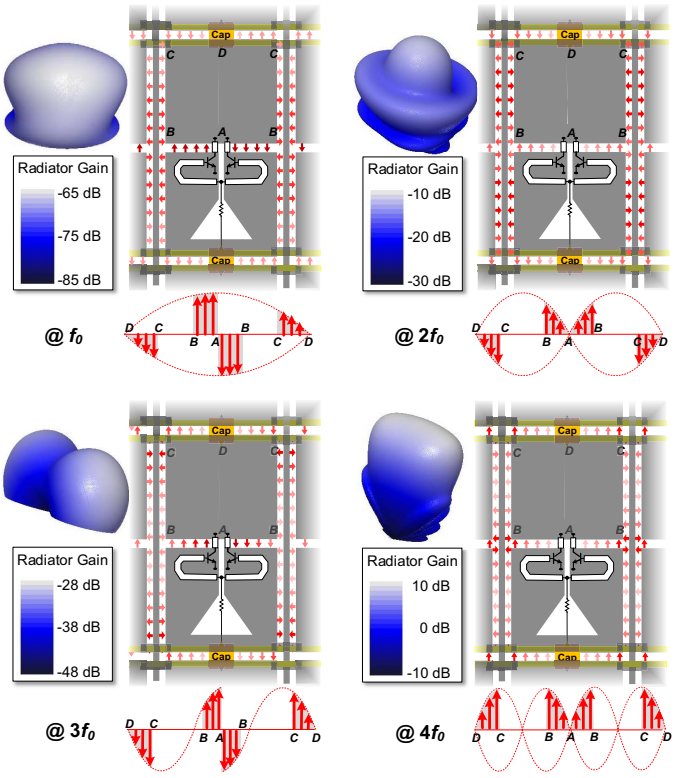

Fig. 4: Distribution and near-field interference of electrical fields in the slots of a radiator at various harmonic frequencies (f_0=250 GHz), as well as the simulated radiator gain and patterns.

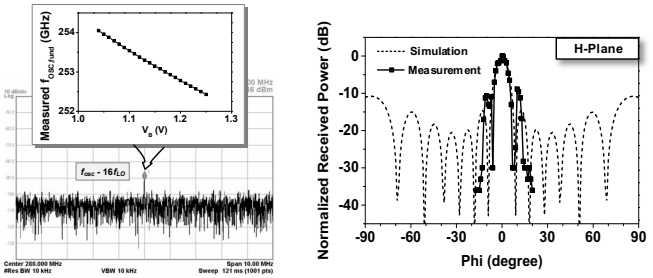

(a) (b)

Fig. 5: (a) Down-converted spectrum of the leaked fundamental (250-GHz) signal. (b) Measured radiation pattern of the 1-THz source.

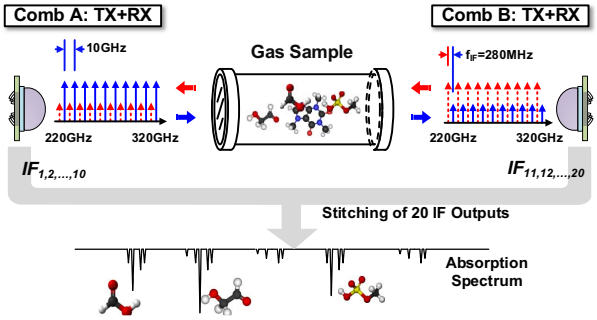

Fig. 6: Dual-frequency-comb, bilateral spectroscopy.

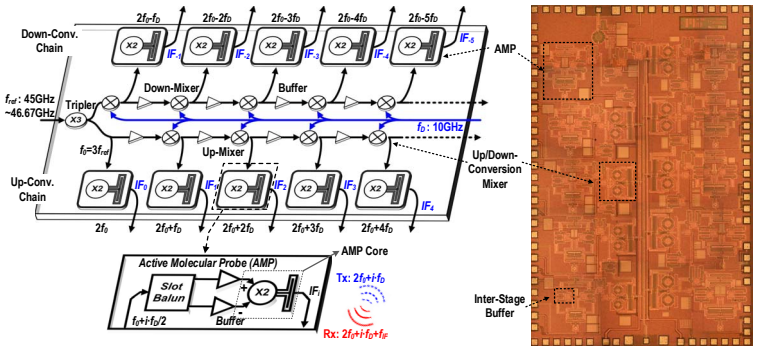

Fig. 7: The architecture and the die photo (area: 2×3 mm^2) of the 220-to-320-GHz comb spectrometer in 65-nm CMOS.

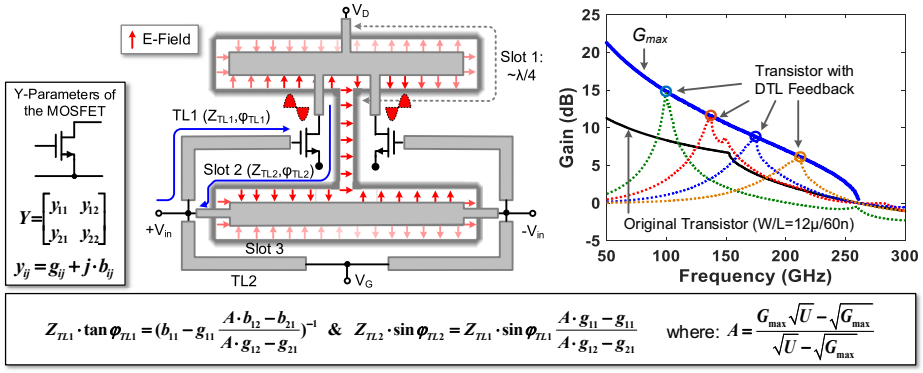

Fig. 8: Operation of the active molecular probing (AMP) core for a differential input signal at fundamental frequency. The design parameters and simulation results of the dual-transmission-line (DTL) feedback are also shown.

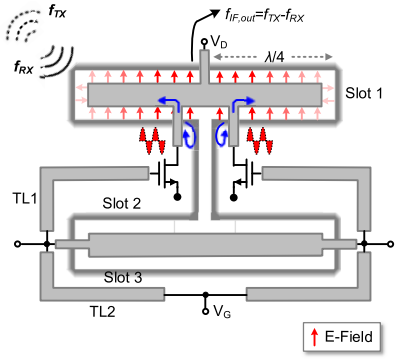

Fig. 9: Measured noise figure of each active molecular probe of the comb spectrometer.

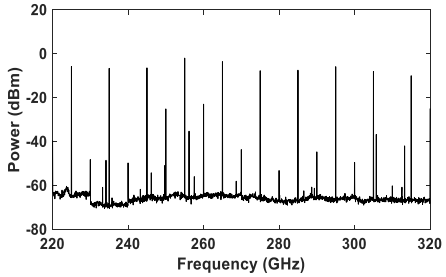

Fig. 10: Measured down-converted comb spectrum using a VDI sub-harmonic mixer for each comb line radiation channel.

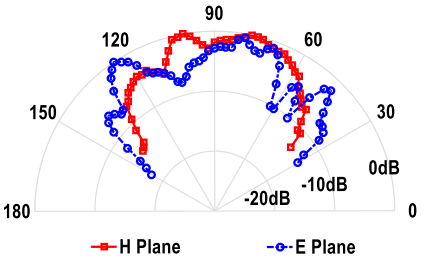

Fig. 11: Measured radiation pattern of one comb line output at 265 GHz.

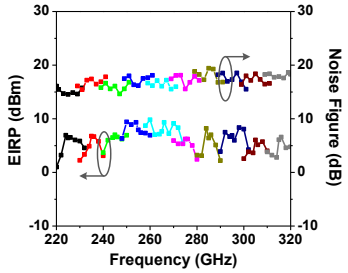

Fig. 12: Measured EIRP and noise figure of each active molecular probe of the comb spectrometer.

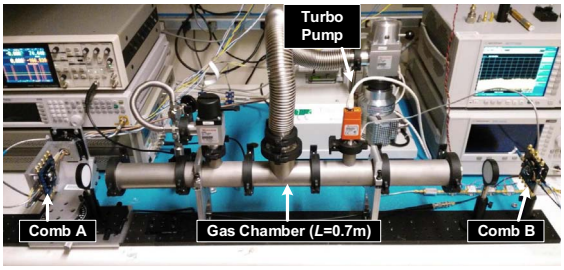

Fig. 13: Experimental setup of the THz rotational spectroscopy using the CMOS dual-comb chipset.

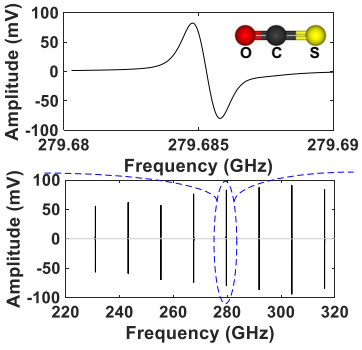

Fig. 14: Measured spectrum of carbonyl sulfide (OCS).

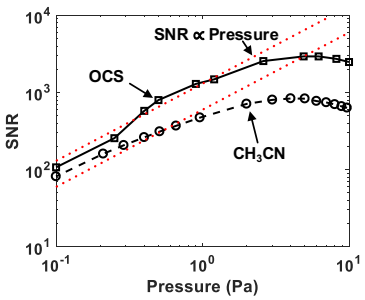

Fig. 15: Spectroscopic $SNR_{v/v}$ at various pressures (τ=1 ms).